UK/KRCEE Doc #: P8.3 2005

Seismic Velocity Measurements at Expanded Seismic Network Sites

Prepared by
Kentucky Research Consortium for Energy and Environment
233 Mining and Minerals Building
University of Kentucky, Lexington, KY 40506-0107

Prepared for
United States Department of Energy Portsmouth/Paducah Project Office
Acknowledgment: This material is based upon work supported by the Department of Energy under Award Number DE-FG05-03OR23032.

UNIVERSITY OF KENTUCKY

January 2005

UK/KRCEE Doc #: P8.3 2005

Seismic Velocity Measurements at Expanded Seismic Network Sites

Prepared by

Principal Investigator: Edward W. Woolery
Department of Earth and Environmental Sciences
University of Kentucky
101 Slone Research Building
Lexington, KY 40506-0053
woolery@uky.edu

Co-Investigator: Zhenming Wang
Kentucky Geological Survey
228 Mining and Mineral Resources Building
Lexington, KY 40506-0107
zmwang@uky.edu

The views and conclusions contained in this document are those of the authors and should not be interpreted as necessarily representing the official policies, either expressed or implied of the Commonwealth of Kentucky.

January 2005

Executive Summary

Structures at the Paducah Gaseous Diffusion Plant (PGDP), as well as at other locations in the northern Jackson Purchase of western Kentucky may be subjected to large far-field earthquake ground motions from the New Madrid seismic zone, as well as those from small and moderate-sized local events. The resultant ground motion a particular structure is exposed from such events will be a consequence of the earthquake magnitude, the structure's proximity to the event, and the dynamic and geometrical characteristics of the thick soils upon which they are, of necessity, constructed. This investigation evaluated the latter. Downhole and surface (i.e., refraction and reflection) seismic velocity data were collected at the Kentucky Seismic and Strong-Motion Network expansion sites in the vicinity of the Paducah Gaseous Diffusion Plant (PGDP) to define the dynamic properties of the deep sediment overburden that can produce modifying effects on earthquake waves. These effects are manifested as modifications of the earthquake waves' amplitude, frequency, and duration. Each of these three ground motion manifestations is also fundamental to the assessment of secondary earthquake engineering hazards such as liquefaction. The expected earthquake ground motions are routinely modeled using one-dimensional linear-equivalent response analyses. The numerical calculation of this soil transfer function on the propagating earthquake wave requires knowledge of the shear-wave velocities, damping ratios, and soil horizon thicknesses. The resultant dynamic properties from this investigation can be immediately used to model scenario design ground motions at the vertical strong motion array. Moreover, magnitude-distance equivalent comparisons of modeled ground motions with measured ground motions at the Paducah vertical strong-motion array (VSAP) can be used to determine and constrain any 2- or 3-dimensional effects not considered in the standard practice one-dimensional modeling techniques.

1.0 Objectives

The purpose of this investigation was to provide each of the Kentucky Seismic and Strong-Motion Network (KSSMN) expansion observatories, VSAP, PAKY, and LVKY (Fig. 1), the following dynamic site characteristics: 1) measured S-wave velocity model (using P-wave measurements to constrain depth where needed), 2) damping ratio, and 3) fundamental site period. The field measurements combined data from *in situ* seismic reflection/refraction walkaway and seismic downhole surveys following the recognized standards-of-practice as described in the general provisions of U.S. Army Corps of Engineers EM 1110-2-1802 [1996], "Geophysical Exploration for Engineering and Environmental Investigations."

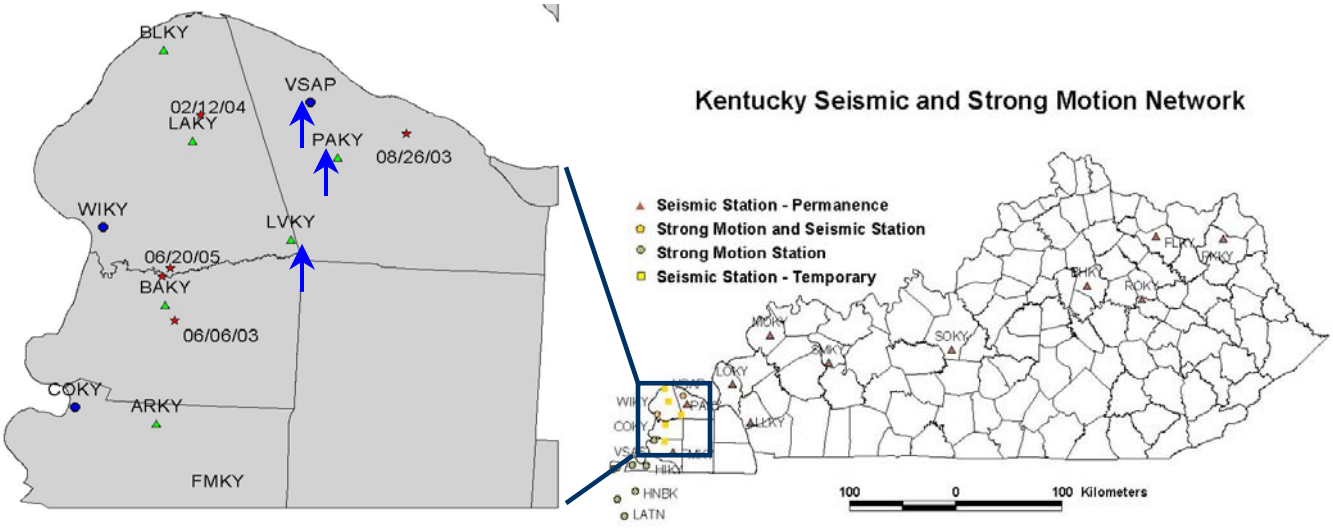

Figure 1. The investigations were performed at three of the Kentucky Strong-Motion and Seismic expansion sites (shown by the blue arrows in the inset) in the Jackson Purchase of western Kentucky (partially outlined by the blue rectangle).

2.0 Significance

The Upper Mississippi Embayment is a large wedge-shaped syncline that dips to the south, and is filled with several tens to several hundreds of meters of unlithified and semi-lithified, post-Paleozoic sediments (Fig. 2). Underlying the embayment, and aligned approximately with its axis is the New Madrid seismic zone (NMSZ), which Cramer (2001) estimated is capable of producing large (> M7) earthquakes at mean-

recurrence intervals of 498 years. The effects of the unlithified sediments in the vicinity of the Paducah Gaseous Diffusion Plant (PGDP) on ground motions from a large far-field NMSZ earthquake or a moderate-sized local earthquake are poorly understood because of the lack of both instrumental records and *S*-wave velocity data for the soil deposits. The soil overburden, as well as the subsurface bedrock topography, can have a significant effect on the earthquake ground motions in the local area. *S*-waves propagating upward through thick layers of unlithified sediments are apt to be amplified and induce resonance at selected periods. Consequently, realistic determination of site response and modeling of earthquake-induced ground motions at and in the vicinity of the PGDP cannot be accurately achieved without the characterization of the dynamic properties and layer thicknesses in the sediments that overlie bedrock at the network observation sites.

The numerical calculation of the soil transfer function that describes the effects of a propagating earthquake wave requires knowledge of the shear-wave velocities, damping ratios, and soil horizon thicknesses. The shear-wave velocity is the most important of the experimental measurements, because the shear-wave velocity can be used to back calculate an elastic unit's quality factor, Q (or damping), and estimate the dynamic site period.

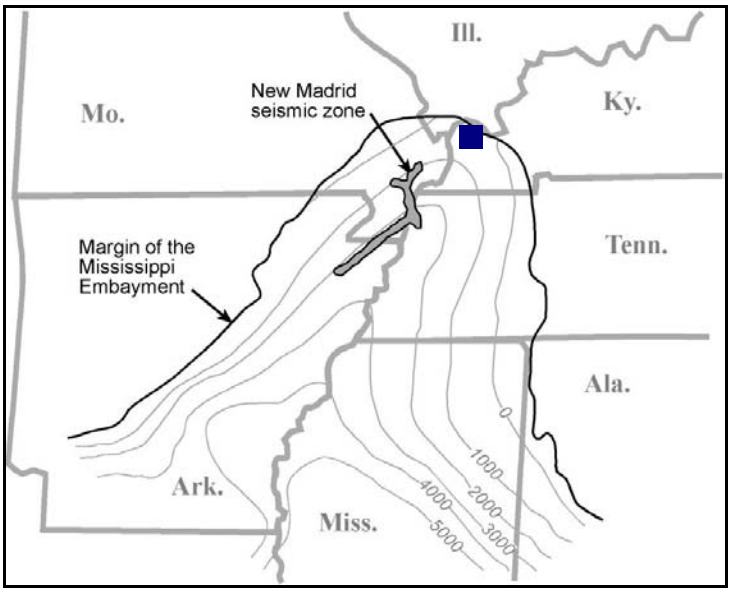

Figure 2. The general study area (blue-filled rectangle) is shown in relation to the New Madrid seismic zone and the Mississippi embayment. The embayment contours show sediment thickness in feet below mean sea level.

3.0 Field Methods

The geophysical survey sites were located at the KSSMN expansion sites described by the coordinates listed below:

VSAP: 37.131N/88.813W

PAKY: 37.068N/88.772W

LVKY: 36.970N/88.829W

Surface refraction surveys at PAKY and LVKY were collected approximately 0.5km from the borehole coordinate because of cultural/natural obstructions.

3.1 Seismic Downhole

The downhole shear-wave measurements were conducted by placing an S-wave energy source on the ground surface 2 meters from the borehole opening with a triaxial geophone array placed at various elevations in the borehole (Fig. 3).

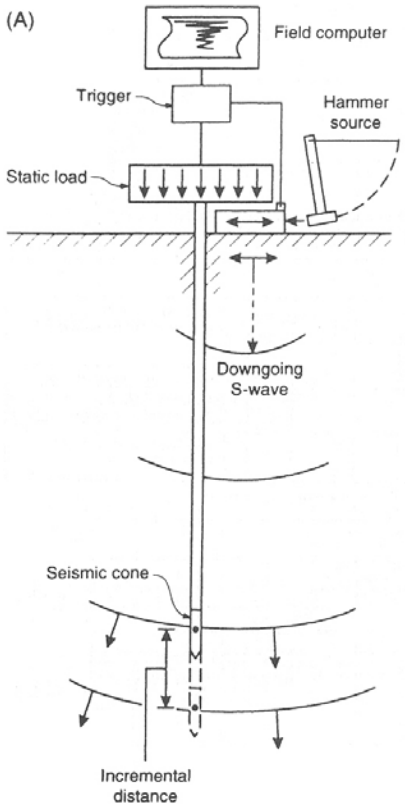

Figure 3. A schematic of a typical field setup used for a downhole seismic test (from Reynolds, 1997).

The downhole survey measures the travel time of the seismic wave from the energy source to various elevations of the geophone. More importantly, the downhole survey forces the seismic wave travel path to traverse all strata between the energy source and receiver; therefore, it has the ability to detect velocity inversion layers. The energy source was a section of steel H-pile struck horizontally by a 1-kg hammer. The hold-down weight on the H-pile was approximately 70 to 80 kg. The flange of the source opposite the side receiving the hammer blow was embedded into slots cut into the surface to improve the energy coupling. The down-hole receiver was a Geostuff model BHG-2c, 14-Hz, 3-component geophone. A geophone to borehole coupling was developed via a motor-driven piston that expanded and contracted a wall-lock spring. At each downhole collection point, shear-wave arrival times were acquired from orthogonal directions (i.e., arbitrary longitudinal and transverse directions) (Fig. 4). This decreased the potential effects associated with repeatability (timing offsets) and preferred axial orientations (anisotropy). The earliest arriving shear wave was assumed to represent the average shear-wave velocity to that depth. Each data collection point was vertically "stacked" 10 to 15 times in order to improve the signal-to-noise ratio.

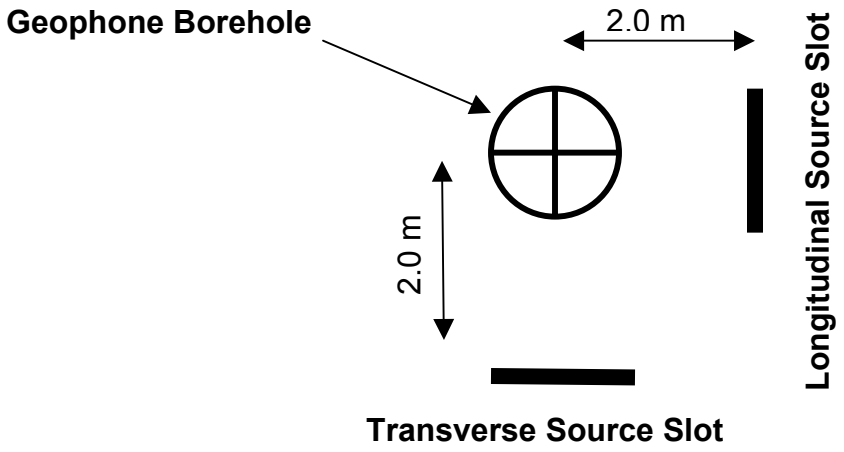

Figure 4. Plan view of the actual downhole seismic survey acquisition geometry.

An initial test of uncorrected polarization was performed to insure that shear waves were properly identified (Fig. 5). Subsequently, individual traces were corrected for polarity, bandpass filtered, gain controlled, and spliced into an overall downhole composite. The

first-break travel-time picks were interactively selected using commercial signal processing software, VISTA 7.0 (Seismic Image Software Ltd., 1995) and the shear-wave velocity profile was subsequently calculated using generic spreadsheet algorithms.

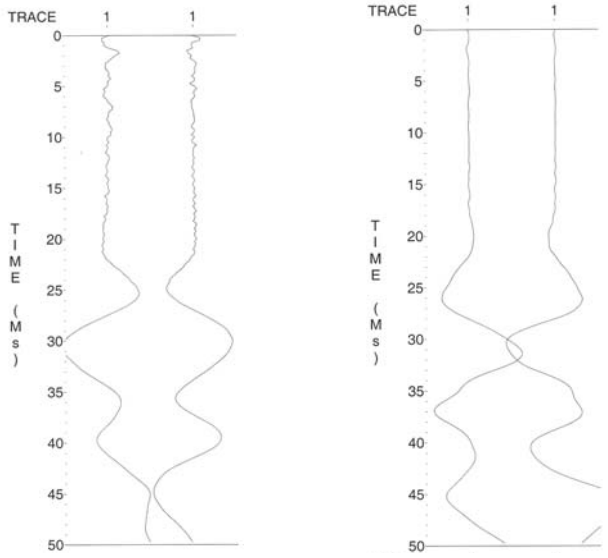

Figure 5. Uncorrected polarity tests were performed on the longitudinal (left) and transverse (right) elements of the downhole geophone in order to insure correct identification of the shear wave.

In addition to the traditional downhole test described above, a "walkaway" vertical seismic profile (VSP) was performed in order to measure the bedrock shear-wave velocity. The energy source, borehole geophone, and processing procedures were identical to the simple downhole test. The difference between the surveys was defined by the geometrical acquisition configuration. The walkaway VSP placed the geophone at the bottom of the borehole (i.e., resting directly on the top of bedrock). Shear-wave energy was placed into the ground at increasing distances from the wellhead in order to develop and record a critically refracted wave along the top of rock. The initial source-wellhead offset was 200 meters. The seismic energy source was "stepped out" at 10-meter increments to a maximum 580-meter source-wellhead offset.

3.2 Seismic Refraction

The seismic refraction survey is a seismic "drilling" technique that samples a specific site by a variety of energy-source to receiver offsets (Fig. 5). The data set defines the two-way travel to the various subsurface refracting (and reflecting) impedance horizons. The

measured travel time and the known array geometry permit the seismic velocity and depth of each subsurface unit to be calculated. The two refraction arrays were collected using twenty-four (24), 30-Hz, horizontally polarized geophones spaced at 3.05 m intervals. The tests were reversed (to correct for non-horizontal horizons), with multiple reciprocity shot points for each line. The seismic energy was generated by 15 horizontal impacts of the 1-kg hammer to a modified H-pile section with a hold-down weight of 75 kg. To ensure the accurate identification of SH-mode events, impacts were recorded on each side of the energy source. By striking each side of the source and reversing the acquisition polarity of the engineering seismograph, inadvertent P- and SV-mode energy will stack in a destructive manner, while SH-mode will stack constructively. Refraction/reflection field records were also processed using commercial signal processing and interpretation software. A band-pass filter and an automatic gain control were applied to the records. No additional processing was necessary.

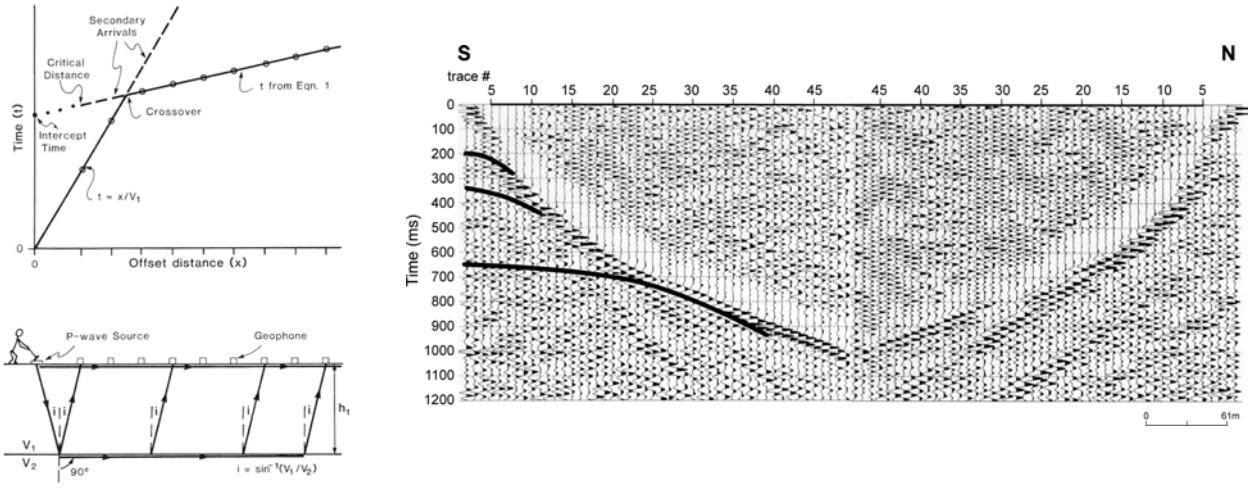

Figure 5. A generalized schematic is shown on the left for the seismic refraction procedure with a simple one layer over infinite half space (from Lankston, 1990). The seismograms on the right are typical multi-layered reversed datasets that exhibit both refraction and reflection events.

4.0 Velocity Results

4.1. VSAP:

The interval shear-wave velocities from the surface to a depth of 100 m ranged between 237 m/s and 618 m/s. These velocities were derived from fair-to-good quality data. The downhole waveform composite and the interpreted model are shown in Figure 6. The

detailed downhole measurements for the sites are given in the composite layer interpretations in Table 1. The results of the "walkaway" VSP are shown in figure 7. Two velocities, 595 m/s and 1630 m/s, were derived from the poor-to-fair quality dataset. These interpreted velocities correlate to the McNairy Formation and bedrock, respectively. The 595 m/s shear-wave velocity for the McNairy Formation is also similar to the interval velocities derived from the downhole survey. A "rubber-banding" technique available in VISTA70 allowed first-arrival time interpolation through areas of poor data quality. No signal was observed (or interpolated) beyond 490 meters, however.

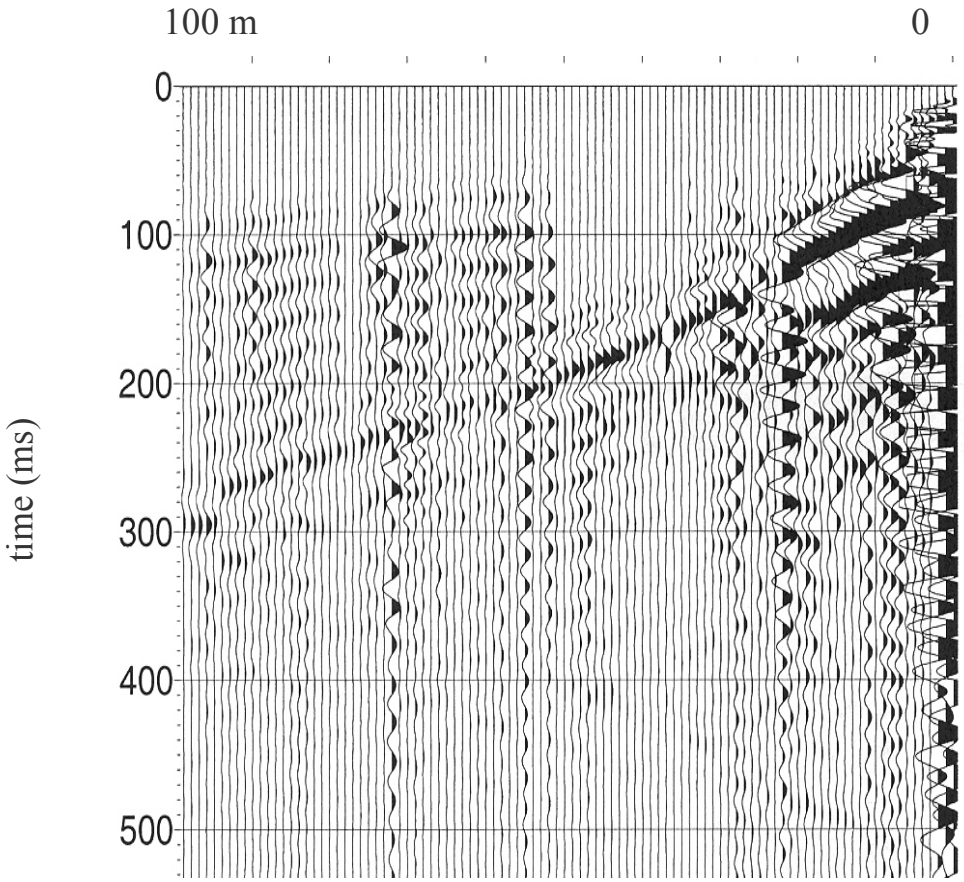

Figure 6a. The downhole s-wave waveform composite.

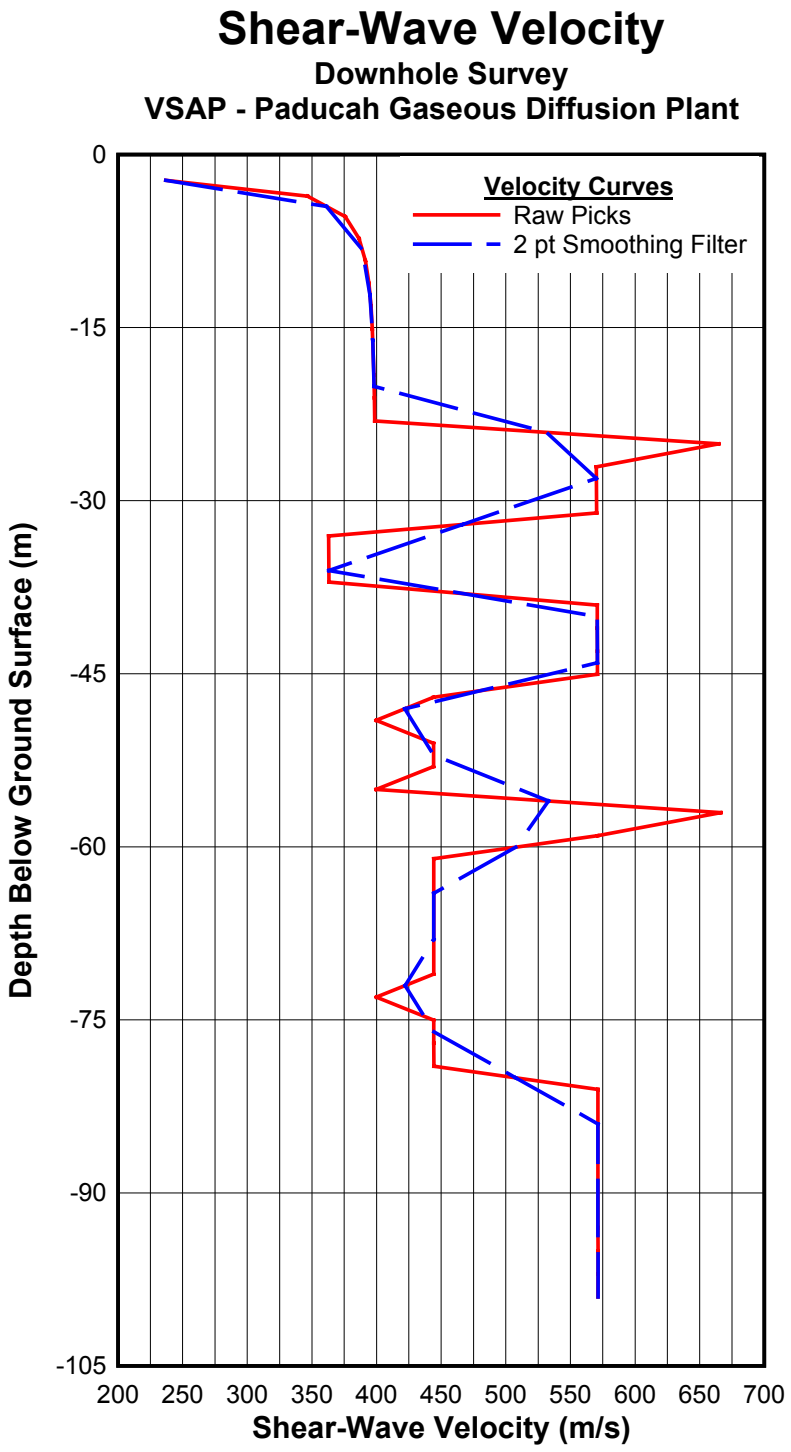

Figure 6b. The resultant raw and smoothed s-wave interval velocity plot.

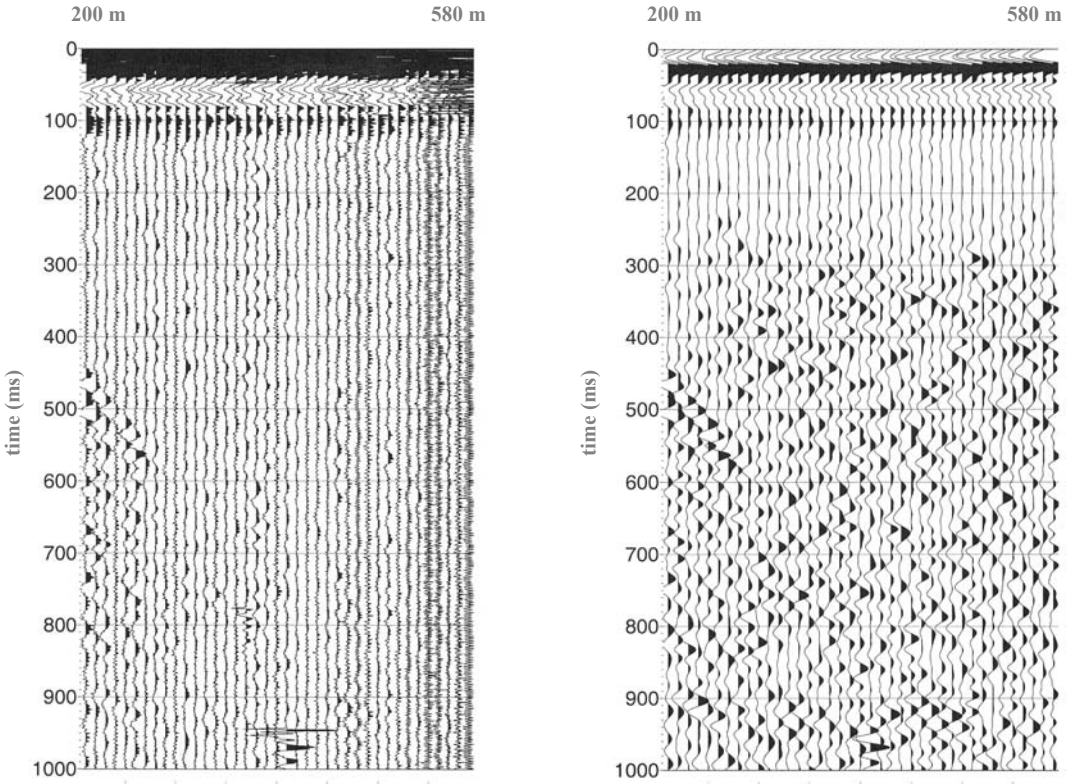

Figure 7a. The composite seismic waveform data are shown for the walkaway VSP survey. The raw and filtered/gained data are shown on the right and left, respectively.

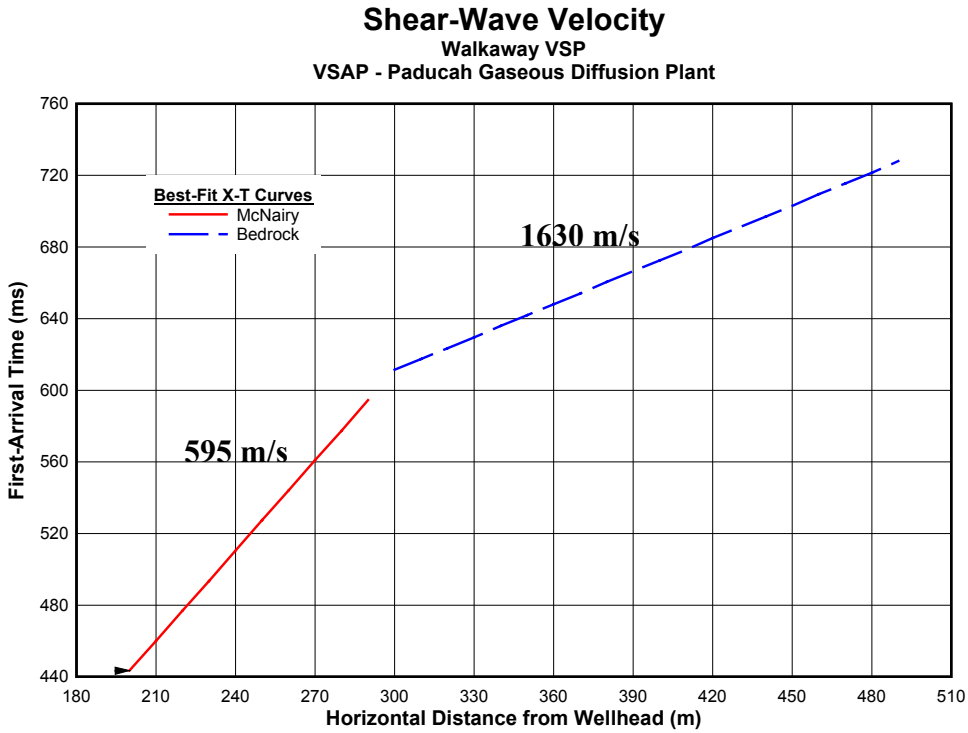

Figure 7. Best-fit curves through the composite seismic waveform data are shown. A "rubber-banding" technique available in VISTA70 allowed first-arrival time interpolation through areas of poor data quality. No signal was seen (or interpolated) beyond 490 meters.

4.2. PAKY:

The shear-wave velocities from the surface to top-of-bedrock at a depth of 161 m ranged between 207 m/s and 448 m/s. These velocities were derived from fair-to-good quality data. The waveform composite and the interpreted model are shown in Figure 8. The composite layer interpretations are also shown in Table 1.

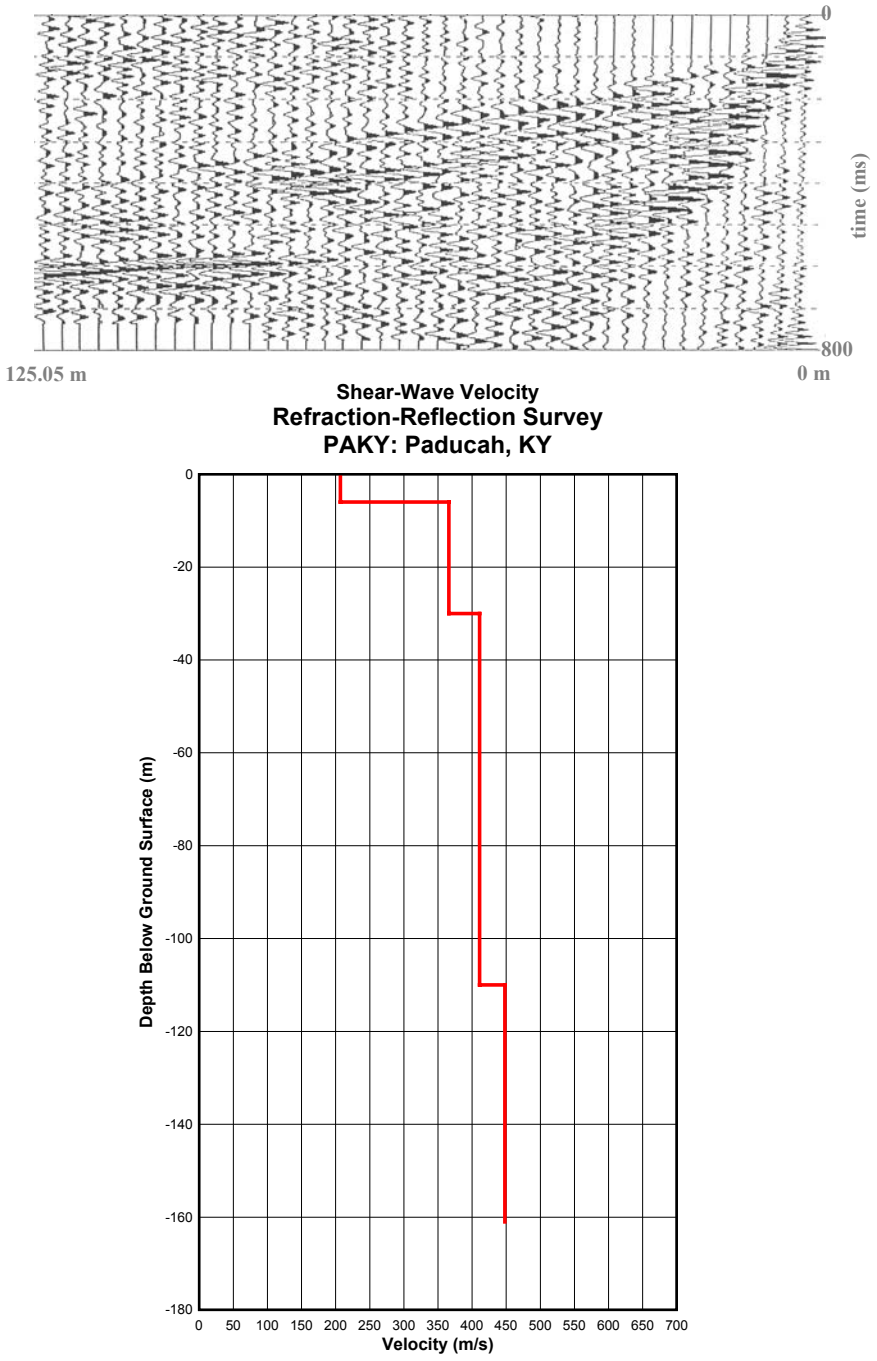

Figure 8. Surface refraction/reflection s-wave survey was performed near PAKY. An example of a composite seismic waveform field file is shown at the top, and the interpreted velocity model is shown at the bottom.

4.3. LVKY:

The shear-wave velocities from the surface to top-of-bedrock at a depth of 125 m ranged between 182 m/s and 618 m/s. These velocities were derived from fair-to-good quality data. The waveform composite and the interpreted model are shown in Figure 9. The composite layer interpretations are also shown in Table 1.

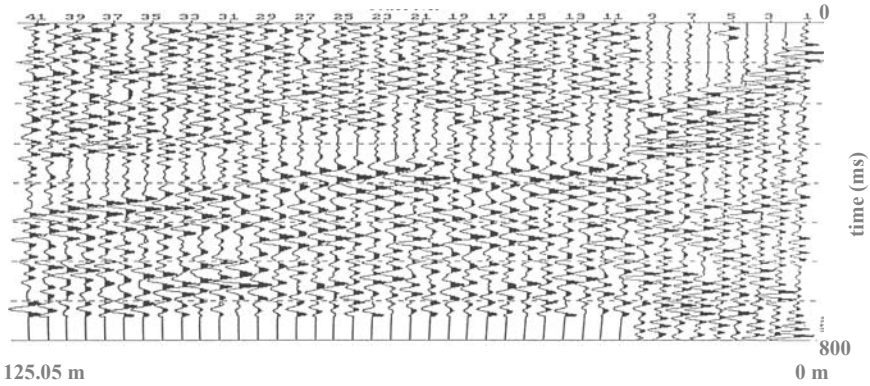

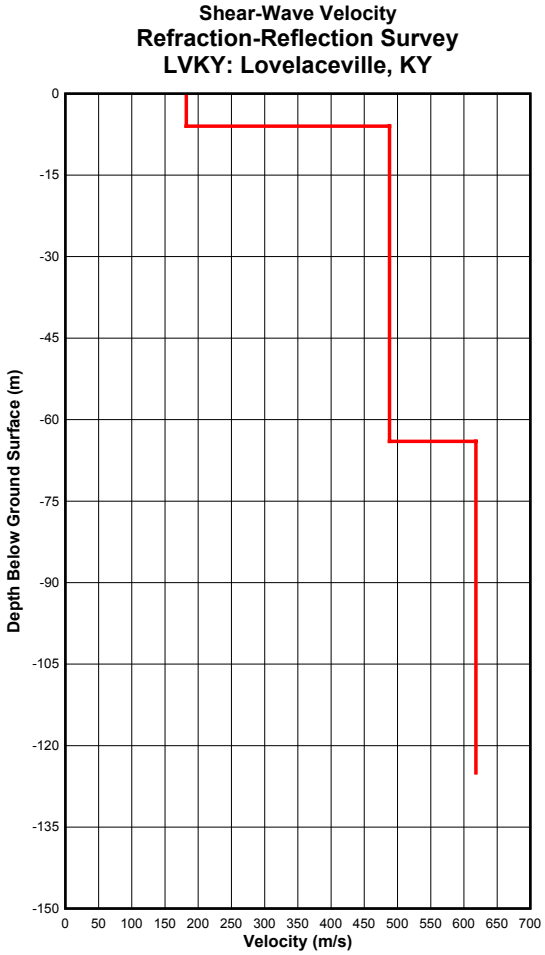

Figure 9. Surface refraction/reflection s-wave survey was performed near LVKY. An example of a composite seismic waveform field file is shown at the top, and the interpreted velocity model is shown at the bottom.

4.0 Damping (δ) and Quality Factors (Q)

Damping (δ) for the soil layers was estimated from the shear-wave velocities using the shear-wave quality factor (Q_S) and the relationship:

$$\delta = (2Q_S)^{-1}$$

which is frequently used for small strains (i.e., 10^{-5} %) when the stress-strain behavior of the soil is approximately linear (Mok et al., 1988). Wang et al. (1994) used a pulse-broadening technique to find that the Q_S of the unlithified soils in the northern Mississippi embayment, including the Jackson Purchase of western Kentucky, could be related to the shear-wave velocity of the soils by the relationship:

$$Q_S = 0.08V_S + 6.99 \pm 12.10.$$

Small strains for the northern Jackson Purchase area were specified in the analysis because any large earthquake is assumed to be in the far-field of the southern or central NMSZ. It is also unlikely that moderate-sized local events will induce nonlinear conditions. The resultant estimates for the damping factors are given in Table 1.

5.0 Dynamic Site Periods

The n^{th} natural frequency of a sediment deposit can be defined as a function of its shear-wave velocity (V_s) and thickness (H):

$$\omega_n \approx \frac{V_S}{H}\left(\frac{\pi}{2} + n\pi\right) \quad \text{where, n = 0, 1, 2, 3, …}\infty.$$

Intrinsic damping of the medium will result in the decrease of the spectral ratio with increasing natural frequency, however. Consequently, the highest spectral ratio will occur approximately at the lowest natural frequency (i.e., first harmonic). Therefore, the fundamental natural frequency can be written as:

$$\omega_0 = \frac{\pi V_S}{2H}.$$

The period (T) that corresponds to the fundamental natural frequency is called the dynamic site period:

$$T_0 = \frac{2\pi}{\omega_0} = \frac{4H}{V_S}.$$

The dynamic site period depends only on the soil thickness (d) and shear-wave velocity (V_S); however, the shear-wave velocity can vary significantly throughout the entire soil deposit. In order to estimate T_0, we defined the bulk shear-wave velocity for the entire soil column by a time-weighted average:

$$\overline{V_S} = \frac{\sum_{i=1}^{n} d_i}{\sum_{i=1}^{n} \frac{d_i}{V_{S,i}}}.$$

The resultant estimates for the dynamic site period are shown in Table 1.

Site	Layer Thickness (m)	Velocity (m/s)	Damping Factor (δ)	Site Period (T_0) (sec)
VSAP	3	237	0.019	0.89
	21	389	0.013	
	8	594	0.009	
	6	363	0.014	
	8	571	0.009	
	10	426	0.012	
	4	618	0.008	
	20	440	0.011	
	20	571	0.009	
	Bedrock	1630*		
PAKY	6	207	0.021	1.61
	24	366	0.014	
	80	411	0.012	
	51	448	0.011	
LVKY	6	182	0.023	1.00
	58	488	0.010	
	61	618	0.008	

6.0 Summary and Recommendations

The refraction and downhole data were collected and analyzed using standards of geophysical practice. Overall, the S-wave downhole and refraction data at the site were of fair to good quality. The long offsets required to observe critical refraction combined with the high attenuation properties of the soil column, resulted in poor-to-fair data

quality for the "walkaway" VSP, however. The calculated results from the tests correlate reasonably well with results of numerous other refraction and downhole datasets collected by the investigators in similar geologic settings. The absolute accuracy of the refraction measurements at sites PAKY and LVKY must be qualified by the theoretical constraints of the potential low-velocity inversion; however, the downhole measurements are sensitive to the low-velocity inversions associated with the interbedded, depositional nature of the soils.

The dynamic site period represents the natural (fundamental) period at which the soil overburden will resonate in the event of an earthquake. In order to lessen the damage potential, engineered structures should be designed so that their natural periods do not coincide with the dynamic site periods. Furthermore, the thickness of the soil deposits and their shear-wave velocities can vary significantly over short distances. Consequently, careful judgment must be exercised in extrapolating these results to other sites. Site-specific investigations should be undertaken to verify or modify the dynamic and geometrical characteristics, particularly for sensitive structures.

7.0 References

Lankston, R.W. ,1990. High Resolution Refraction Seismic Data Acquisition and Interpretation, *Soc. Explor. Geophys., Investigations in Geophysics no. 5*, Stanley Ward ed., Volume 1: Review and Tutorial, p. 45–75.

Reynolds, J.M., 1997, An Introduction to Applied and Environmental Geophysics, John Wiley and Sons, New York, 796 pp.

Seismic Image Software Ltd., 1995, VISTA, V–7.0.

U.S. Army Corps of Engineers, 1996, Geophysical Exploration for Engineering and Environmental Investigations, EM-1110-2-1802, Springfield, VA.

Wang, Z., Street, R., Woolery, E., and Harris, J., 1993, Q_s estimation for unconsolidated sediments using first-arrival SH-wave refractions: Journal of Geophysical Research, v.99, p. 13543-13551.